# Alignment of the CMS silicon tracker

**Gero Flucke on behalf of the CMS Collaboration**
Deutsches Elektronen-Synchrotron, Hamburg, Germany
E-mail: gero.flucke@desy.de

**Abstract.** The CMS all-silicon tracker consists of 16 588 modules with 25 684 sensors in total. In 2010 it has been successfully aligned using tracks from cosmic rays and proton-proton collisions, following the time dependent movements of its innermost pixel layers. In 2011, ultimate local precision is achieved by determining sensor curvatures in addition to module shifts and rotations, challenging the alignment procedure to determine about 200 000 parameters. This is achieved in a global fit approach using MILLEPEDE II with the General Broken Lines track model. Remaining alignment uncertainties are dominated by systematic effects that bias track parameters by an amount relevant for physics analyses. These effects are controlled by including information about the $Z$ boson mass in the fit.

## 1. Introduction

The inner tracker of the CMS detector [1] at the LHC is completely based on silicon sensor technology. The tracker is placed inside a large solenoid providing a magnetic field of 3.8 T. The CMS coordinate system is defined such that the $z$-axis coincides with the nominal beam line. The radial distance from the $z$-axis is denoted as $r$. The polar angle $\theta$ is measured from the positive $z$-axis and the azimuthal angle $\phi$ is measured in the plane perpendicular to it. The innermost part of the tracker ($r < 20$ cm) consists of 1440 pixel modules. The barrel (BPIX) and forward (FPIX) pixel sub-detectors are surrounded by 15 148 strip modules up to $r < 110$ cm, arranged in four sub-detectors: the Tracker Inner and Outer Barrels (TIB and TOB), the Tracker Inner Disks (TID), and the Tracker End-caps (TEC). All sub-detectors are concentrically arranged around the $z$-axis. Modules at $r > 60$ cm contain two daisy-chained sensors, leading to 24 244 strip sensors in total.

To fully exploit the single hit resolution of down to 9 $\mu$m for pixel and of 23 to 60 $\mu$m for strip sensors, the positions of the sensors must be known to a precision of a few micrometers. This can best be achieved by track-based alignment algorithms. For the CMS tracker these have been applied using tracks from cosmic ray events [2], from a mixture of cosmic ray and first LHC collision events [3], and from complete 2010 data taking [4]. Based on the experience with these data and having collected a large sample of high momentum tracks in 2011, alignment development focuses now on systematic effects biasing reconstructed track parameters.

This article first recalls the principle of track-based alignment and explains the technological improvements needed to face the large amount and the required precision of the alignment parameters that are needed at CMS. Then the main results of the 2011 alignment campaign and their validation are presented, followed by a summary.

## 2. Track-based alignment

### *2.1. Principle*

Track-hit residual distributions are generally broadened if the assumed positions and orientations of the silicon modules differ from the true ones. Following the least squares approach, alignment algorithms minimise the squares of normalised residuals, summing over many tracks. If the (hit or virtual) measurements $m_{ij}$ with uncertainties $\sigma_{ij}$ are independent, the minimised function is

$$\chi^2(\mathbf{p},\mathbf{q}) = \sum_{j}^{tracks} \sum_{i}^{measurements} \left( \frac{m_{ij} - f_{ij}\left(\mathbf{p},\mathbf{q}_j\right)}{\sigma_{ij}} \right)^2 \tag{1}$$

where $f_{ij}$ is the track model prediction at the position of the measurement, depending on the alignment ($\mathbf{p}$) and track ($\mathbf{q}_j$) parameters. In the global fit approach as implemented in the MILLEPEDE II program [5], $\chi^2(\mathbf{p},\mathbf{q})$ is minimised after linearising $f_{ij}$. This leads to the normal equations $\mathbf{C}\mathbf{a} = \mathbf{b}$ with $\mathbf{a}^T = (\mathbf{p},\mathbf{q})$, i. e. all alignment parameters $\mathbf{p}$ and all parameters of all $n$ used tracks $\mathbf{q}^T = (\mathbf{q}_1,\ldots,\mathbf{q}_n)$. Due to the special structure of $\mathbf{C}$, block matrix algebra facilitates the reduction of this large system of equations to a smaller one for the alignment parameters only,

$$\mathbf{C}'\mathbf{p} = \mathbf{b}'. \tag{2}$$

$\mathbf{C}'$ and $\mathbf{b}'$ sum contributions from all tracks. For each track a matrix equation $\mathbf{C}_j\mathbf{q}_j = \mathbf{b}_j$ has to be solved and $\mathbf{C}_j^{-1}$ needs to be calculated.

### *2.2. The general broken lines fit*

Since multiple scattering effects are relevant in the CMS tracker, they have to be taken into account in the track model. This can be achieved by increasing the number of parameters for a charged particle in the magnetic field to $n_{par} = 5 + 2n_{scat}$, e. g. adding two deflection angles for each of the $n_{scat}$ thin scatterers.[1] Since the expectation value of these scattering angles $\beta$ is zero, virtual measurements $\beta = 0 \pm \sigma_\beta$ are added for each of them with $\sigma_\beta$ according to the track momentum and the traversed material. For cosmic ray tracks this often leads to $n_{par} > 50$. Since in the general case the effort to calculate $\mathbf{C}_j^{-1}$ is proportional to $n_{par}^3$, a significant amount of computing time would be spent to calculate $\mathbf{C}_j^{-1}$ and thus $\mathbf{C}'$ and $\mathbf{b}'$. The progressive Kalman filter fit as used in CMS track reconstruction avoids the $n_{par}^3$ scaling, but cannot be used with MILLEPEDE II that requires the complete covariance matrix $\mathbf{C}_j^{-1}$.

The General Broken Lines track refit [6] provides $\mathbf{C}_j^{-1}$, but avoids the $n_{par}^3$ scaling by defining a track parametrisation with local meaning. These parameters are $\mathbf{q}_j = (\Delta\frac{q}{p}, \mathbf{u}_1, \ldots, \mathbf{u}_{(n_{scat}+2)})$, where $\Delta\frac{q}{p}$ is the change of the charged inverse momentum and $\mathbf{u}_i$ are the two-dimensional offsets to a reference trajectory in local systems at each scatterer and at the first and last measurement (figure 1). Predictions $\mathbf{u_{int}}$ for hit measurements are derived by interpolating between scatterers and the multiple scattering angles are determined from triplets of adjacent scatterers. This locality of all track parameters (except $\Delta\frac{q}{p}$) results in $\mathbf{C}_j$ being a bordered band matrix with band width $m \leq 5$ and border size $b = 1$. Using root free Cholesky decomposition, the effort to calculate $\mathbf{C}_j^{-1}$ and $\mathbf{q}_j$ is reduced to $\propto \left(n_{par}^2 \cdot (m+b)\right)$ and $\propto \left(n_{par} \cdot (m+b)^2\right)$, respectively.

The MILLEPEDE II program detects bordered band matrices while constructing $\mathbf{C}'$ and $\mathbf{b}'$, saving a factor 7 in CPU time for refitting cosmic ray tracks. The equivalence of Kalman filter and General Broken Line fits is shown for simulated muon tracks in figure 2 [6].

[1] For thin scatterers as used in CMS track reconstruction, the trajectory offsets induced by multiple scattering can be ignored. If a scatterer is thick, it can be treated as two thin scatterers.

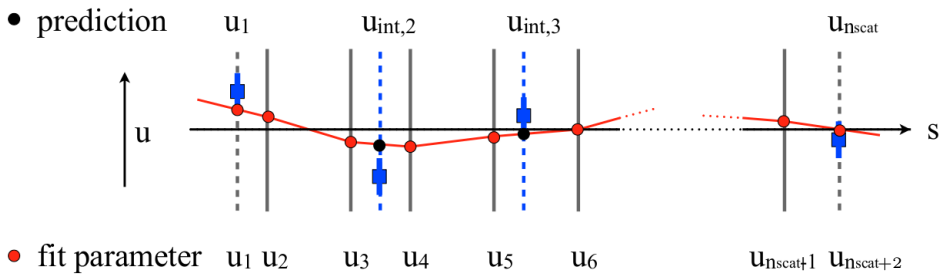


**Figure 1.** General Broken Lines track parametrisation along the path $s$ of a reference trajectory. Dashed lines indicate the measurement planes, solid lines the thin scatterers, blue squares the measurements, black circles the trajectory predictions and red circles the fitted track parameters.

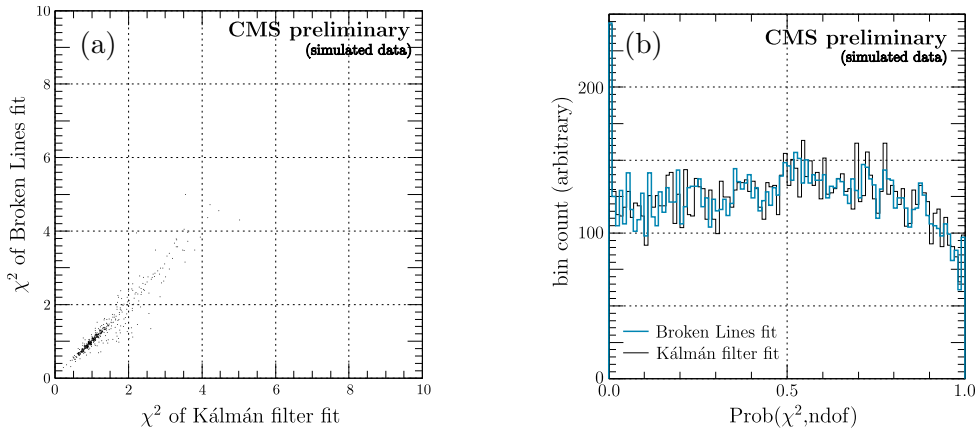


**Figure 2.** Correlation of $\chi^2/ndf$ values of single tracks (a), and probability value distributions (b), comparing the General Broken Lines with the Kalman filter fit.

*2.3. Choice of alignment parameters*

Previous alignment approaches treated the silicon modules as flat surfaces. Up to 5 (6) degrees of freedom per strip (pixel) module had been determined. But tracks with large angles relative to the module normal, e. g. tracks from the interaction point with small angles relative to the beam line, and cosmic ray tracks, are sensitive to small flatness deviations. These variations arise from silicon sensors being curved and, for strip modules with two sensors in a chain, from their relative misalignment. Therefore the vector of alignment parameters $\mathbf{p}$ has been extended to up to 9 degrees of freedom per sensor (instead of 6 per module). The sensor shape is parametrised as a sum of modified (orthogonal) Legendre polynomials up to order 2 where up to order 1 is equivalent to the rigid body parameters (figure 3).

Further alignment parameters are used for time dependent shifts and rotations of BPIX layers and FPIX half disks while the modules are kept fixed within these structures using constraints. Nine periods of time with relevant movements have been determined using the track-vertex residual monitoring introduced in section 3.2. In total, more than 200 000 alignment parameters have been determined in a common fit.

*2.4. Momentum changing weak modes*

Minimising residuals is not sufficient to find the alignment corrections $\mathbf{p}$. Systematic movements of silicon sensors and changes of track parameters can balance each other without changing the overall $\chi^2$, biasing the track parameters. Avoiding these so-called weak modes is the major alignment challenge once local precision is reached using many tracks from collisions. The best

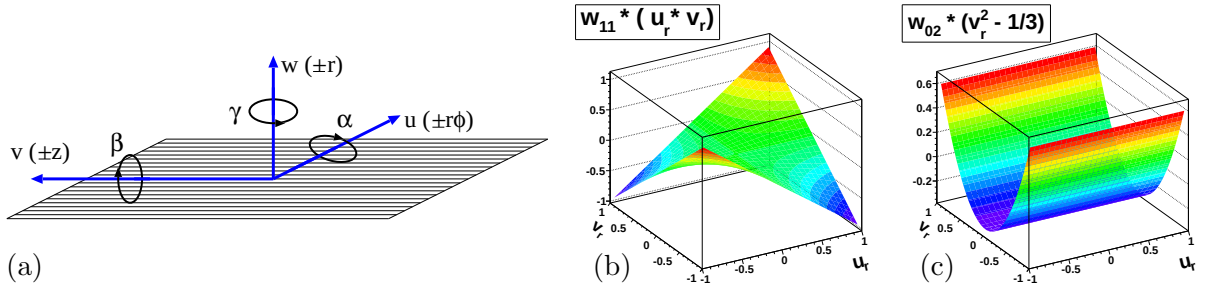


**Figure 3.** Sensor alignment parametrisation: The Cartesian coordinate system $uvw$ and the rotations $\alpha\beta\gamma$ for the six rigid body parameters, where $u$ and $v$ lie in the sensor plane and $u$ is the more precisely measured direction (a). Two of the three polynomials to describe deviations from the flat plane, where $u_r = \frac{2u}{l_u}$ and $v_r = \frac{2v}{l_v}$ are the relative positions on the plane with length $l_u$ and width $l_v$ (b and c).

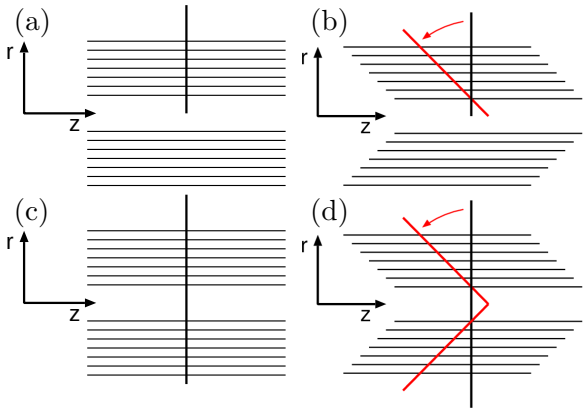


**Figure 4.** Using cosmic ray tracks avoids the telescope weak mode as explained in the text.

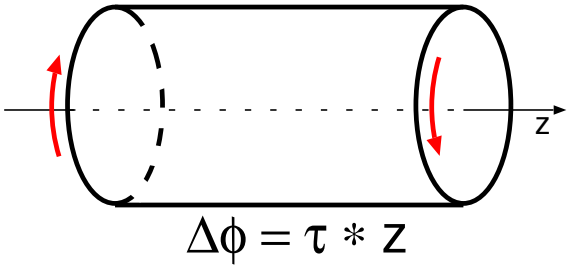


**Figure 5.** The twist weak mode.

handle to control these weak modes is their dependence on the data used in equation (1).

Making use of cosmic ray tracks is a key ingredient, controlling several distortions that are weak modes if using only tracks originating from the interaction region. Such a track is sketched in figure 4(a) together with a cut through the tracker along the $z$-axis. A so-called telescope distortion ($z$-position of the module biased proportionally to its radial coordinate, $\Delta z \propto r$) does not change the track-hit residuals, but clearly biases the track direction as illustrated in figure 4(b). A cosmic track connects the upper and lower part of the tracker as shown in figure 4(c). This prevents the telescope distortion, since either the track would be kinked, which is prevented by the track parametrisation, or the residuals would increase as can be seen from figure 4(d).

A systematic distortion $\Delta\phi \propto z$ (figure 5) is only partially controlled using cosmic ray tracks. This so-called twist biases the curvature of high momentum tracks. The transverse momentum measurement is oppositely affected as a function of the pseudorapidity $\eta = -\ln(\tan\theta/2))$ for tracks of positively and negatively charged particles. The effect on the reconstructed mass of a resonance decaying into two muons depends on the charge and $\eta$ of the decay products. The sensitivity on the twist depends on the difference of the longitudinal momenta of the muons, i.e. is largest for large differences in $\eta$. Thus the bias is more severe for heavy resonances produced with smaller boosts, like the $Z$ boson.

To avoid this twist effect, information about the mass of the $Z$ boson is used in the alignment

fit as follows. A common parametrisation for the two trajectories of the decay tracks is found [7]. Instead of $2 \times 5$ parameters (plus those accounting for multiple scattering), the nine common parameters are the position of the decay vertex, the momentum of the $Z$ candidate, two angles defining the direction of the muons in the rest-frame of the $Z$ boson, and its mass. The nominal $Z$ mass is added as a virtual measurement with an uncertainty corresponding to the standard deviation of the $Z$ lineshape around the peak position. In the sum on the right hand side of equation (1) the two individual tracks are replaced by the common fit object. The corresponding $\mathbf{C}_j$ has a border size $b = 9$. It should be noted that this approach implies a rigorous implementation of a vertex constraint as well since the parametrisation forces the tracks to a common vertex.

### *2.5. Optimisation of memory usage and speed*

The task of the MILLEPEDE II program is to setup matrix equation (2) and to solve it to get the alignment parameters $\mathbf{p}$.

The matrix $\mathbf{C}'$ is symmetric and its elements need to be stored in double precision for accuracy. For 200 000 alignment parameters this would require 160 GB of RAM that are not easily affordable. But the matrix is rather sparse, so only non-zero elements need to be stored, reducing the storage need. Since these elements are usually close to each other, further compression is reached by bit-packed addressing of non-zero blocks in a row. Finally, some matrix elements sum contributions of only a few tracks, e. g. cosmic ray tracks from rare directions. For these elements single precision storage is sufficient.

The most important ingredients that speed up MILLEPEDE II are the following. The iterative MINRES algorithm [8] is used to solve equation (2). Besides the speed gain compared to invert $\mathbf{C}'$ this makes the sparse storage mentioned above possible. As already explained in section 2.2, bordered band matrices $\mathbf{C}_j$ are automatically detected when setting up equation (2). Finally, CPU intense parts as MINRES and track fits are parallelised using OpenMP® [9]. Reading data from local disk and memory access are the remaining bottlenecks. To reduce the time needed for reading, MILLEPEDE II can read compressed input and caches the information of many tracks to reduce the number of disk accesses.

## 3. CMS tracker alignment 2011

The alignment of the CMS tracker in 2011 was performed based on data collected until end of June, using about 15 million loosely selected isolated muon tracks, 3 million low momentum tracks, 3.6 million cosmic ray tracks (collected between LHC fills, during collisions and before collision data taking) and 375 thousand muon track pairs from $Z$ boson decays. Within a few hours, 246 parallel jobs produced the compressed input files of in total 46.5 GB, containing residuals, uncertainties and derivatives for the linearised track model $f$. More than 200 000 alignment parameters were determined in the final minimisation program. The constructed matrix $\mathbf{C}'$ contained 31% non-zero off-diagonal elements. With a compression ratio of 40% this fitted well into 32 GB of memory. The input files were read 13 times: twice to setup the addressing for the reduced memory usage, four times to run MINRES with subsequently tighter rejection of bad tracks, and seven times for one dimensional line searches after the MINRES calls. Using eight threads on an Intel® Xeon® L5520 with 2.27 GHz, the CPU usage was 44.5 h with a wall clock time of only 9:50 h.

### *3.1. Modules with curved sensors*

The parametrisation with polynomials describes the sensors very well. This can be seen in figure 6 where the offsets $dw$ are calculated from the residuals in $u$ and the track angle $\psi$ from the sensor normal in the $uw$ plane. For an alignment with the flat sensor assumption, a parabolic shape is seen that vanishes taking into account the additional parameters.

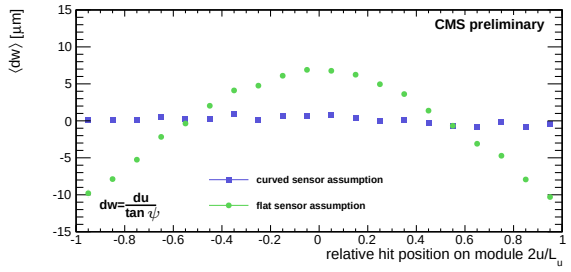


**Figure 6.** Average track-hit offsets perpendicular to the sensor plane across TIB modules.

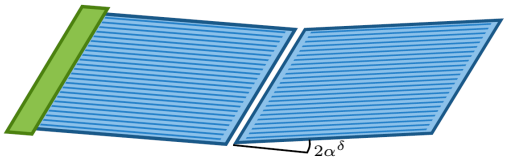


**Figure 7.** Sketch of a strip module with two sensors in a chain.

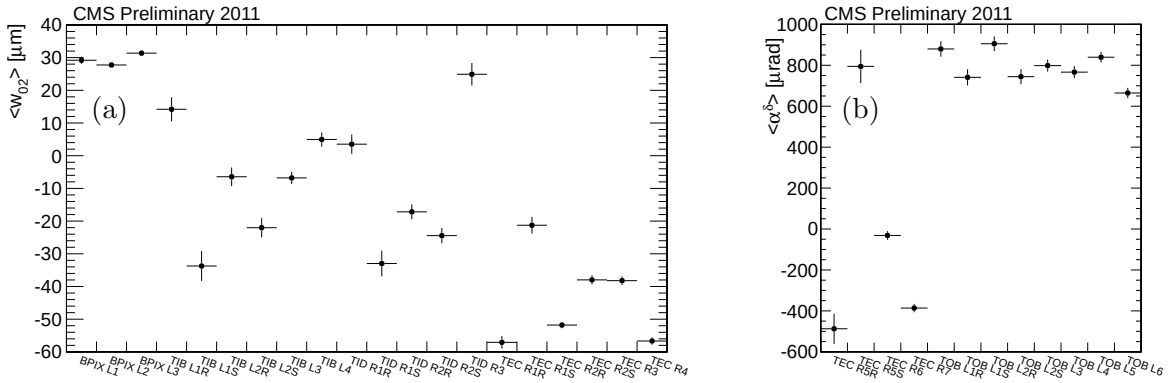


**Figure 8.** Curvature along the local $v$ coordinate for single sensor modules (a) and half difference of the rotation around local $u$ for double sensor modules (b), averaged for all modules of same type and similar mounting. The module radii increase with layer (ring) number L (R).

Figure 8 shows average values of some of the determined parameters describing deviations from flat modules. A curvature along the local $v$ axis of $w_{02} = 30$ $\mu$m in the BPIX means that the sensor position in $w$ at the edges ($v_r = \pm 1$) differs by 20 $\mu$m from the average. Modules in the first layer with largest $|z|$ are crossed by tracks from the interaction point under large angles relative to the sensor normal. Therefore hit position corrections of around 100 $\mu$m have to be applied. These are quite relevant compared to the hit resolution of down to 9 $\mu$m.

For TOB modules, the largest deviations from flatness result from the kink between the two sensors (figure 7). A size of $\alpha^\delta = 0.8$ mrad results in a deviation of up to 40 $\mu$m in $w$.

While figure 8 shows average values to demonstrate the module and mounting type dependence, the variances of these parameters are relevant. For $w_{02}$ they range from 10 $\mu$m in the BPIX to 50 $\mu$m in the TIB and for $\alpha^\delta$ from 0.8 mrad in the TOB to 2 mrad in the TEC. Strip sensor curvatures are expected due to the single sided processing and are requested to be below 100 $\mu$m [1]. This requirement is fulfilled for the majority of the modules, but not for the tails of the distributions.

High momentum tracks from the interaction region cross the strip modules under small angles relative to the module normal. Therefore sensor curvatures have only a small effect. This is different for cosmic ray tracks that cross the tracker with a large closest distance to the beam line, $d_0$. This is demonstrated in figure 9: The larger $d_0$, the larger the average track angle from the module normal, leading to degraded fit results for the flat module assumption. If curvature parameters on sensor level are determined, the average fit probability is almost flat as

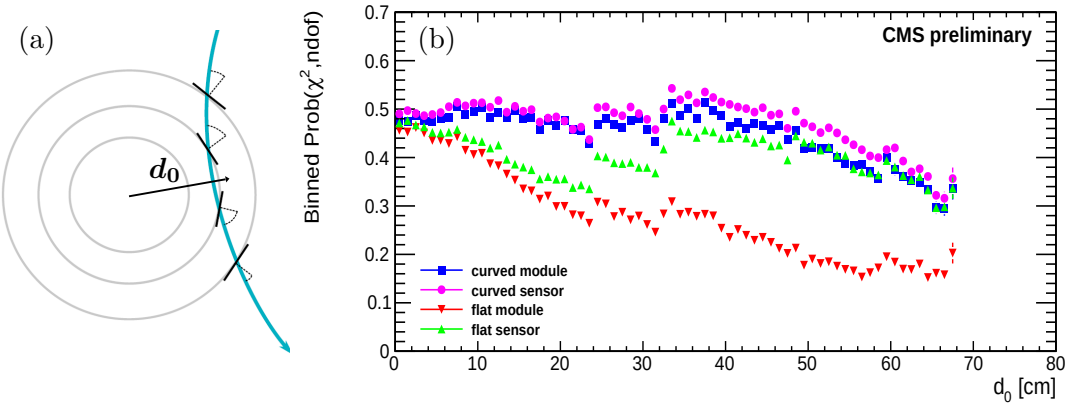


**Figure 9.** Illustration of a cosmic ray track passing the tracker with large $d_0$ (a) and the average fit probability as a function of $d_0$ for different module shape parametrisations (b).

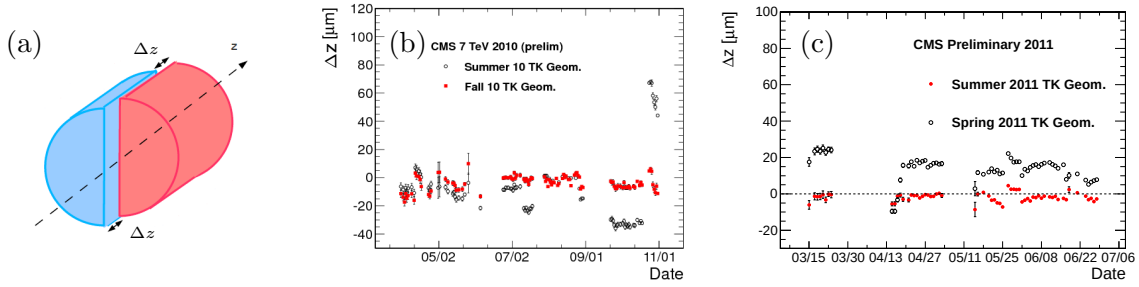


**Figure 10.** The relative misalignment of the two pixel half barrels along the beam line ($\Delta z$, a) is monitored versus time using track-vertex residuals for 2010 (b) and 2011 (c). Black open circles (red dots) refer to the situation before (after) re-alignment, respectively.

a function of $d_0$ up to 50 cm, thus improving substantially the consistency between tracks from the interaction point and cosmic rays. The latter are invaluable to control weak modes in the alignment procedure.

*3.2. Time dependence of large structures of the pixel detector*

Unbiased track-vertex residuals are used to monitor the position of the two pixel half barrels relative to each other. Each primary vertex is refitted after removal of one of its tracks. This is repeated for each track of the vertex. The track-vertex residuals $\Delta z$ along the beam line are averaged as a function of the polar angle $\phi$ of the track. A difference of the mean values for tracks stemming from the one half barrel or the other indicates a relative misplacement. Jumps of up to 100 $\mu$m are seen before alignment in figure 10. After the alignment with time dependent parameters for the positions and orientations of large pixel structures, the remaining half barrel separations are well below 10 $\mu$m, a value that has no effect on the alignment sensitive $b$-tagging algorithms.

*3.3. Control of momentum changing weak modes*

Systematic momentum biases for tracks with high momenta have been investigated using events with a $Z$ boson decaying into oppositely charged muons. The dependence of the position of the mass peak as a function of the pseudorapidity $\eta$ and the polar angle $\phi$ of the positively charged muon is shown in figure 11. Without using the $Z$-mass information in the alignment, a large

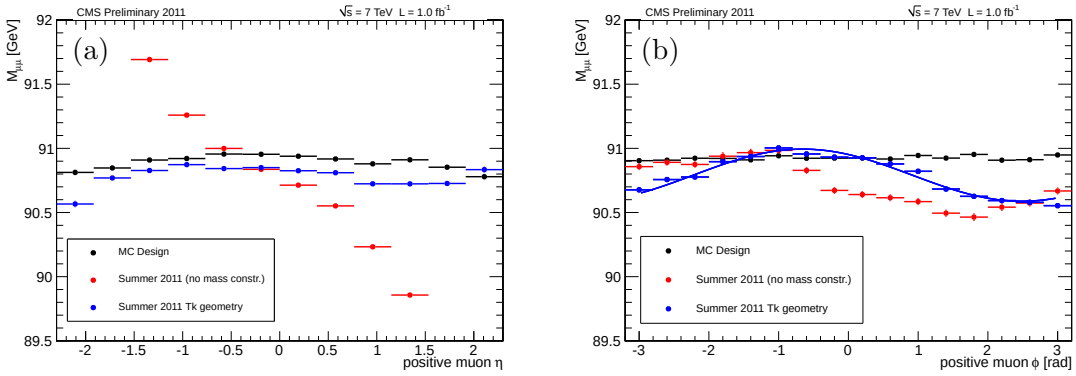


**Figure 11.** Reconstructed mass peak position for $Z \to \mu^+\mu^-$ decays as a function of $\eta$ (a) and $\phi$ (b) of the $\mu^+$, for detector simulations with perfect alignment (black) and for 2011 data aligned with and without special treatment of the $Z$ events (blue and red, respectively).

$\eta$-dependence is observed. It can be related to a twist in the alignment result. In contrast, using this information in the alignment fit as described in section 2.4, the remaining spread of $Z$-mass peak values is almost as small as in the detector simulation with perfect alignment. The reason for the small overall offset between simulation and data and for the sine wave-like dependence on $\phi$ are currently under investigation.

Investigations of the ratio of the energy reconstructed in the hadronic calorimeter and the track momentum for well isolated positively and negatively charged hadron tracks have confirmed the results obtained using $Z$ events, and thus serve as an independent cross check.

## 4. Summary

Recent alignment results for the CMS silicon tracker have been determined using the global fit approach of track-based alignment with the Millepede II program. The use of the General Broken Lines track model makes a rigorous treatment of multiple scattering effects possible and substantially reduces the computing time to set up the large matrix equation of the alignment procedure. Parallelisation of the CPU intense parts of Millepede II and sophisticated storage of the large sparse matrix are further key ingredients to facilitate the determination of more than 200 000 alignment parameters in 9:50 h wall clock time for the final fit, using eight threads and less than 32 GB memory.

This large number of parameters is needed to describe deviations from the flat module assumption and therefore significantly improves the consistency between tracks from the interaction point and cosmic rays. Also tracks passing pixel modules under large angles profit from taking into account the sensor curvature. Movements of larger structures of the pixel detector are taken care of by a time dependence of their alignment parameters, validated using residuals between tracks and their primary vertex.

Inclusion of cosmic ray tracks in the alignment procedure is not sufficient to control all weak modes biasing the curvatures of high momentum tracks. Making use of the mass of the $Z$ boson as an external information reduces the variation of the position of the reconstructed $Z \to \mu^+\mu^-$ mass peak as a function of the direction and charge of its decay products to well below 500 MeV. This remaining dependence is currently being studied in detail, profiting from a fast turnaround due to the speed and modest memory requirements of the alignment procedure using Millepede II with the General Broken Lines track model.

## References


[1] CMS Collaboration 2008 *JINST* **3** S08004
[2] CMS Collaboration 2010 *JINST* **5** T03009
[3] Lampén T 2011 *J. Phys.: Conf. Ser.* **331** 032043
[4] Draeger J 2011 *Track based alignment of the CMS silicon tracker and its implication on physics performance* Ph.D. thesis Universität Hamburg (available from `http://www.physnet.uni-hamburg.de`)
[5] Blobel V 2006 *Nucl. Instr. and Methods* **A566** 5–13
[6] Blobel V, Kleinwort C and Meier F 2011 *Comput. Phys. Commun.* **182** 1760–3
[7] Widl E and Frühwirth R 2007 *Representation and estimation of trajectories from two-body decays* CERN-CMS-NOTE-2007-032
[8] Paige C and Saunders M 1975 *SIAM Journal on Numerical Analysis* **12**(4) 617–29
[9] `http://openmp.org`